AN IMPROVED NETWORK MODEL FOR EDDY CURRENT PROBLEMS

Chi-Chung WONG

Department of Communication and Electronic Engineering
Royal Melbourne Institute of Technology
GPO Box 2476V, Melbourne
Vic., 3001
Australia

ABSTRACT. *This paper describes improvements in modelling Maxwell's equations in two dimensions using the electrical network analogue. Two network models are described with major emphasis placed on diffusion dominated problems. The first one is the combined fine-coarse mesh approach which was initially developed for the method of transmission-line modelling (TLM). The combined fine-coarse mesh technique is then modified by introducing controlled sources at the interfacing between the fine and the coarse mesh. Several numerical experiments, including one with both a conducting region and free space, are used to study the two models. They are also compared with the standard network analogue using a regular meshing. Numerical results are compared with analytical or published data. In all cases, SPICE (or PSPICE) has been used to solve the resulting network analogues.*

1. INTRODUCTION

In 1944 Kron [1] derived an electrical circuit equivalent of Maxwell's equations and subsequently many researchers had used electrical analogues to simulate Maxwell's equations [2-4]. In general, the electrical analogue is built around R, L and C components and the appropriate electrical quantities measured experimentally. With the advent of digital computers, numerical methods such as the finite-difference and finite-element [5] became popular and the use of experimental methods became unattractive. However, it is sometimes desirable to have a physical electrical network analogue for the field region to be modelled and in addition, standard network solver can be used to solve the resultant network analogue without the need of a special finite-element program, for example. Solutions can be sought without the prior knowledge of numerical analysis/methods. In this paper, SPICE[1] (or PSPICE[2]) which is now a *de facto* standard circuit simulator in electronic engineering, is used to solve the resulting network analogue. Another advantage of the network analogue is that it can be used to develop another class of numerical routine, namely the method of transmission-line modelling (TLM) [6]. In principle, SPICE can also be used to implement the transmission-line equivalent of Maxwell's equations, however, this will not be discussed here, because the routine used in SPICE is relatively inefficient for solving transmission-line problems.

The electrical analogue with lumped passive elements is in fact a variant of the finite-difference scheme (in particular with the method of lines) where the space is discretized with a mesh of finite mesh size and the time is left continuous. One major problem associated with this method (and the finite-difference) is that a large number of cells are needed if a regular meshing is used to cover the entire field region. To reduce the number of cells, an irregular meshing can be used [7] as shown in Fig. 1. This approach cannot drastically reduce the total number of cells since some regions outside the area of interest (or where the field gradient is not very steep) still need fine spacings. Another disadvantage of using an irregular meshing is that it is less straightforward to implement and is inherently less accurate [8]. To overcome these problems, the multigrid algorithm has been introduced. This method has been used in finite-difference [9,10] and been successfully applied to the method of TLM for transient diffusion problems [11]. This technique solves two (or more) networks; one with a coarse-mesh grid and the other with a fine-mesh grid. The coarse

[1]SPICE stands for *Simulation Program with Integrated Circuit Emphasis*.
[2]A registered trademark of MicroSim Corporation.

grid overlaps the fine grid (Fig. 2). The coarse grid network is first solved and the appropriate information transferred to the fine grid network and vice versa. Regular cells are commonly used although irregular cells can also be used. In order to reduce the memory requirement, computing time and the interpolation process needed in the multigrid technique, a combined fine-coarse mesh method has been proposed [12]. This arrangement is shown in Fig. 3, where it can be seen that the field region is covered with a combination of fine and coarse but regular cells. The interface between the fine and coarse cell is connected by a "busbar" (Fig. 3a). Therefore, it is only necessary to solve one network and the need to store (and transfer) different sets of information is eliminated. The major drawback of this approach is that accuracy is sacrificed because positions "a", "b" and "c" of Fig. 3a are forced to have the same potential. In this paper a new network model is proposed. The new model is based on the combined fine-coarse mesh technique but the disadvantage associated with this method is eliminated. This is achieved by breaking the "busbar" and use controlled sources at the interface (Fig. 3b). The performance of the original fine-coarse mesh approach and the proposed topology is studied in detail and compared with the standard technique which utilises cells of equal mesh size.

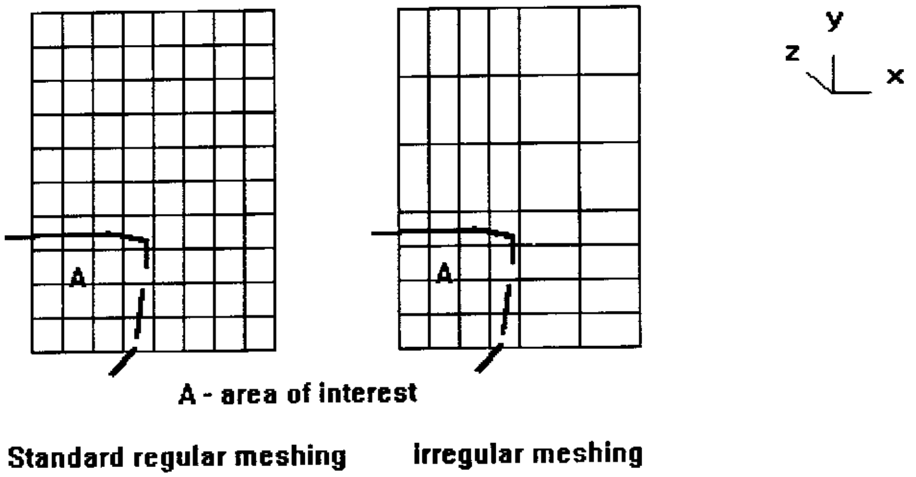

Fig. 1 Typical mesh arrangements.

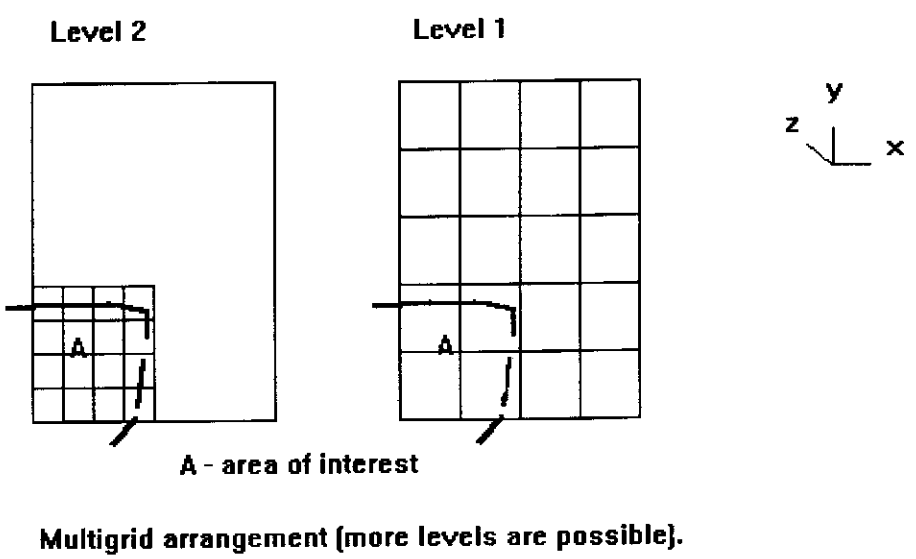

Fig. 2 A multigrid arrangement with two levels shown.

2. THE IMPROVED NETWORK MODEL FOR MAXWELL'S EQUATIONS

2.1 Equivalence between field and network quantities

Consider a typical regular network cell shown in Fig. 4a, the describing equations are

$$\begin{aligned}
&\frac{\partial iy}{\partial y}+\frac{\partial ix}{\partial x}=-c\frac{\partial vz}{\partial t}-gvz\\
&\frac{\partial vz}{\partial x}=-rix-l\frac{\partial ix}{\partial t}\\
&\frac{\partial vz}{\partial y}=-riy-l\frac{\partial iy}{\partial t}
\end{aligned}\qquad(1)$$

where l, r, g and c are the inductance, resistance, conductance and capacitance in per unit length respectively.

Maxwell's equations in two dimensions are (assuming that there is only one component of the H-field)

$$\begin{aligned}
&-\frac{\partial Ex}{\partial y}+\frac{\partial Ey}{\partial x}=-\frac{\partial B}{\partial H}\frac{\partial Hz}{\partial t}\\
&\frac{\partial Hz}{\partial x}=-\sigma Ey-\varepsilon\frac{\partial Ey}{\partial t}\\
&\frac{\partial Hz}{\partial y}=+\sigma Ex+\varepsilon\frac{\partial Ex}{\partial t}
\end{aligned}\qquad(2)$$

where σ, ε and $\partial B/\partial H$ are the conductivity, permittivity and differential permeability of the medium respectively; all units are in per unit length. Comparing eqs. (1) and (2), the following equivalence can be drawn

$$\begin{aligned}
&Hz=vz\ ;\ Ex=-iy\ ;\ Ey=ix\ \textit{and}\\
&\sigma=r\ ;\ \varepsilon=l\ ;\ \frac{\partial B}{\partial H}=c\ ;\ g=0
\end{aligned}\qquad(3)$$

Therefore, an interconnected network of Fig. 4a forms a space discrete model of Maxwell's equations. The resulting network may be solved by various methods. For example, SOR (successive overrelaxation) can be used for steady-state problems. For transient problems, a set of first order ordinary differential equations can be derived and the solution obtained by integration using schemes such as the Runge-Kutta. Alternatively, the time can be further discretized using finite-difference; this is similar to the finite-difference time-domain method. More conveniently, the network may be solved by standard circuit simulators, such as PSPICE which is used in the paper. In this case, it is a simple matter to generate an input file describing the interconnections of the cells shown in Fig. 4a.

2.2 The improved network topology

One major drawback of the network equivalent (and the finite-difference method) is that a large number of cells are needed for typical problems if regular fine cells are used to cover the entire field region. In many cases, fine cells are used in regions where the field variation is less steep. A number of modifications have been proposed as reviewed in the *Introduction*. Among the various methods, the fine-coarse mesh approach, which has been proven to be a viable alternative to the multigrid technique, is the most straightforward to implement. It is only necessary to provide a number of subcircuits (each representing a regular network cell of a given mesh size) for PSPICE. However, this method assumes that the potentials (=H-field) at "a", "b" and "c" are identical (see Fig. 3a). This assumption may be unacceptable at high frequencies, during the initial transient phase or for some special cases. This problem is eliminated by breaking the busbar and replace it by three controlled sources as shown in Fig. 3b. Parameters associated with each of these sources may be determined as shown below.

Using Taylor series expansion and with reference to Fig. 3b, v(z) can be determined in terms of v(z-1) and v(z+1):

$$v(z)=\frac{p(v(z+1))+q(v(z-1))}{p+q}-\frac{1}{2}K(\frac{\partial^2 vz}{\partial^2 y})+O(h^3)\qquad(4)$$

where

$$K=pqh^2\ \textit{and}\ \frac{\partial^2 vz}{\partial^2 y}=\frac{\partial B}{\partial H}(\sigma\frac{\partial vz}{\partial t}+\varepsilon\frac{\partial^2 vz}{\partial^2 t})\qquad(5)$$

If $p = q = 0.5$ and the region is diffusion dominated, eq. (4) becomes

$$\begin{aligned}
v(z)&=0.5(v(z-1)+v(z+1))\\
&-0.125h^2(\frac{\partial B}{\partial H}\sigma\frac{\partial vz}{\partial t})+O(h^4)
\end{aligned}\qquad(6)$$

Eq. (6) has a better error term. Therefore, it is recommended that the coarser mesh size should double the preceding one. Likewise, equations (similar to eq. (4)) can be derived for v(z-1) and v(z+1).

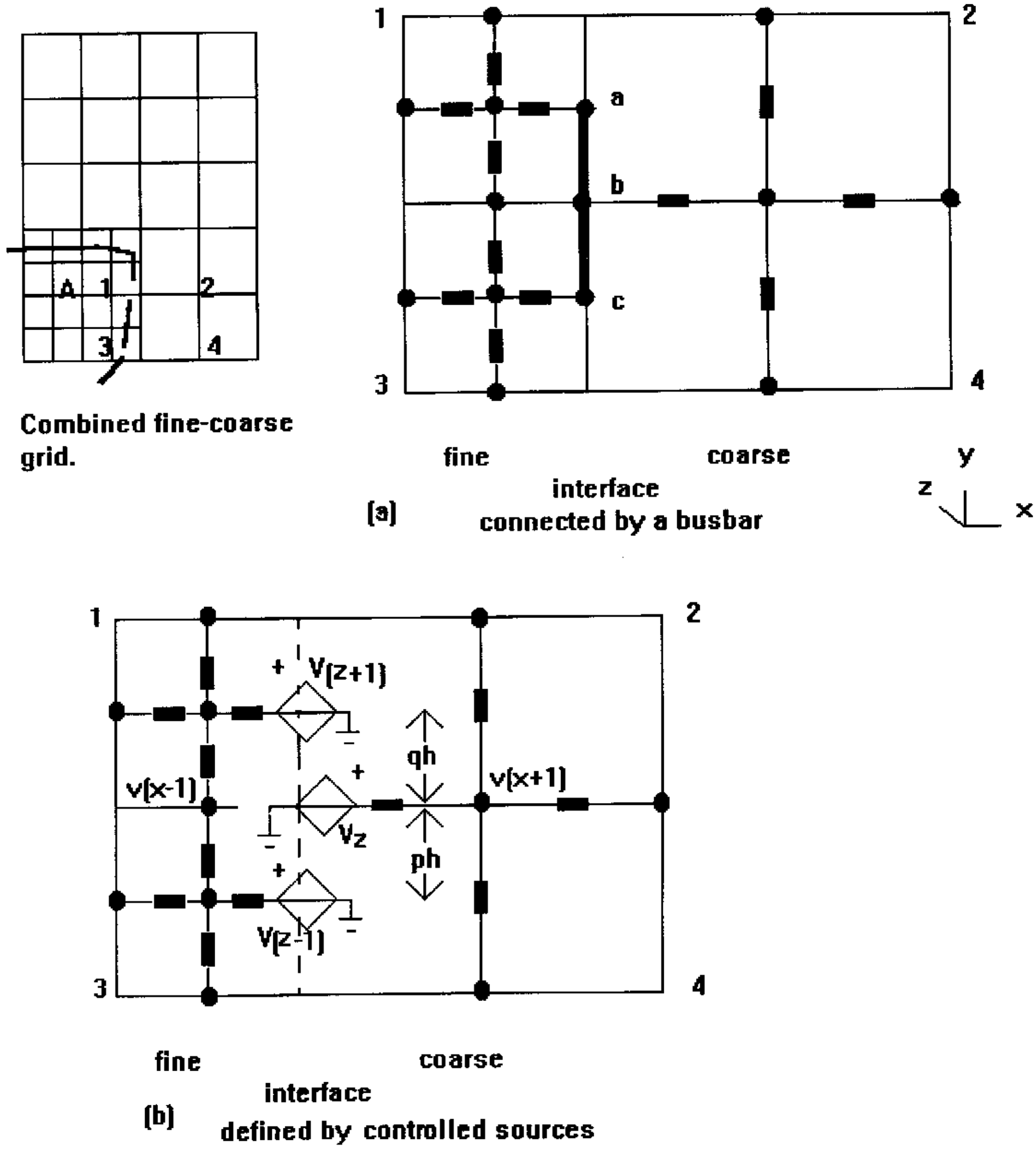

Fig. 3 The combined fine-coarse mesh model and the improved model.

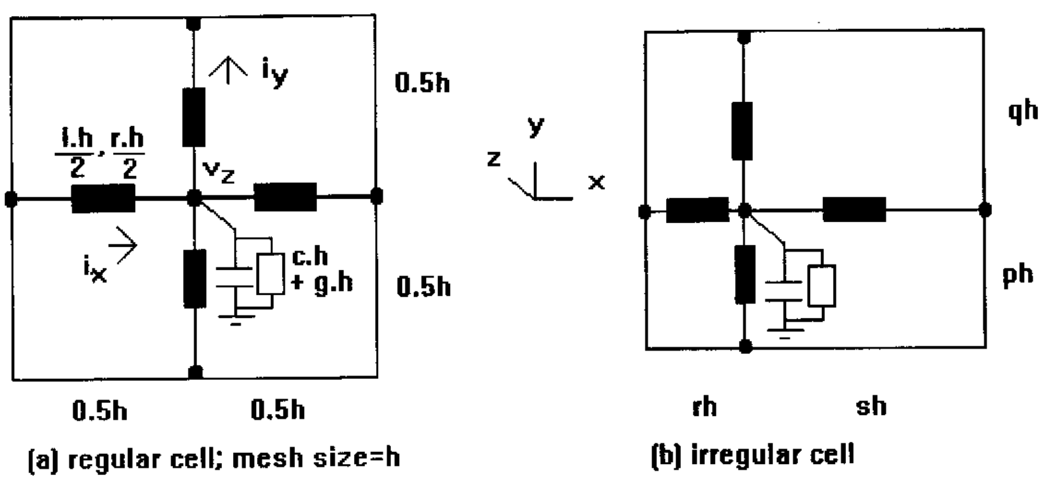

Fig. 4 Typical irregular and regular cells.

The first term of eq. (6) can be easily implemented in PSPICE with controlled sources, however, an additional subcircuit built from a pure inductor (or capacitor) circuit is required to model the second term. This is illustrated in Fig. 5 where the inductor value (L) equals $0.125h^2\sigma(\partial B/\partial H)$.

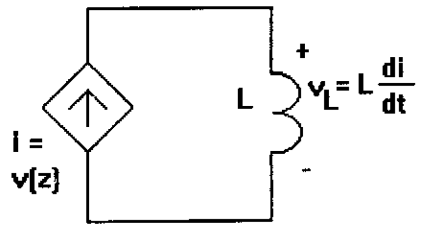

Fig. 5 A subcircuit model for the second term of eq. (6).

The accuracy of eq. (6) may be improved if v(x-1) and v(x+1) are included in the interpolation. Eq. (6) becomes:

$$v(z) = 0.333(v(z-1) + v(z+1)) + 0.222v(x-1)$$
$$+0.111v(x+1) - 0.0833h^2(\frac{\partial B}{\partial H}\sigma\frac{\partial v_z}{\partial t}) \qquad (6a)$$

However, initial results show that the improvement gained in using eq. (6a) is marginal for the examples discussed in the following section and therefore only eq. (6) is used for the improved model.

3. RESULTS

3.1 Flux penetration into a long bar due to an axial H-field

Figure 6 shows the cross-section of a long square bar subjected to the excitation of an axial H-field (H_z). The rise of the magnetic field is determined at two representative positions ("a" and "b_1") when H_z is an impact excitation. Due to symmetry, only one-eighth of the region (for example, OAB) is solved. In the fine mesh region, the mesh size, h, is set to W/8, whereas h = W/4 for the coarse mesh region. For convenience, normalised units and all default settings of PSPICE have been used.

Figure 7 shows the results from the different network models, and they are compared with the exact solution. Both fine-coarse mesh models provide results which are very close to the regular fine mesh model (within 1% for the period shown) but the computing time is cut by at least 50%. The improvement in efficiency is dependent on the "size" of the problem and a better gain can be achieved for larger problems.

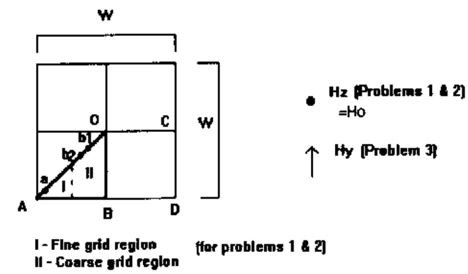

Fig. 6 A long square bar subjected to external H-field excitation.

Accuracy of the network models is best assessed by their corresponding frequency responses. PSPICE provides an efficient way to generate the frequency response curves of the various models. The results are shown in Figures 8a and 8b. The problem is similar to the first case, except that the excitation is sinusoidal and that only steady-state solutions are sought.

It can be seen that the response curves of the new model and the regular fine mesh model are all very close for position "a". The original combined fine-coarse mesh result trails slightly behind. At position "b_1", all three frequency response curves are similar with the original combined fine-coarse model stands out marginally. It should be noted that for the latter case, h = 1/4. A further error analysis is shown in Table 1 where the rms error for the different models are calculated. (Note that the default tolerance of PSPICE is 0.1% and therefore, the errors calculated below are mainly due to the modelling process.)

Table 1 shows that the new model improves the accuracy by approximately 50% (or better) when compared with the original fine-coarse mesh arrangement at position "a". No advantage is observed at the other position, however, both show an improvement over the regular mesh model since fine-mesh information are available to the coarse mesh. The relatively poor accuracy at position "b_1" is not reflected in the transient curves (Fig. 7) because the high frequency components are highly attenuated at this position. This shows that fine cells are not essential at this region for transient studies.

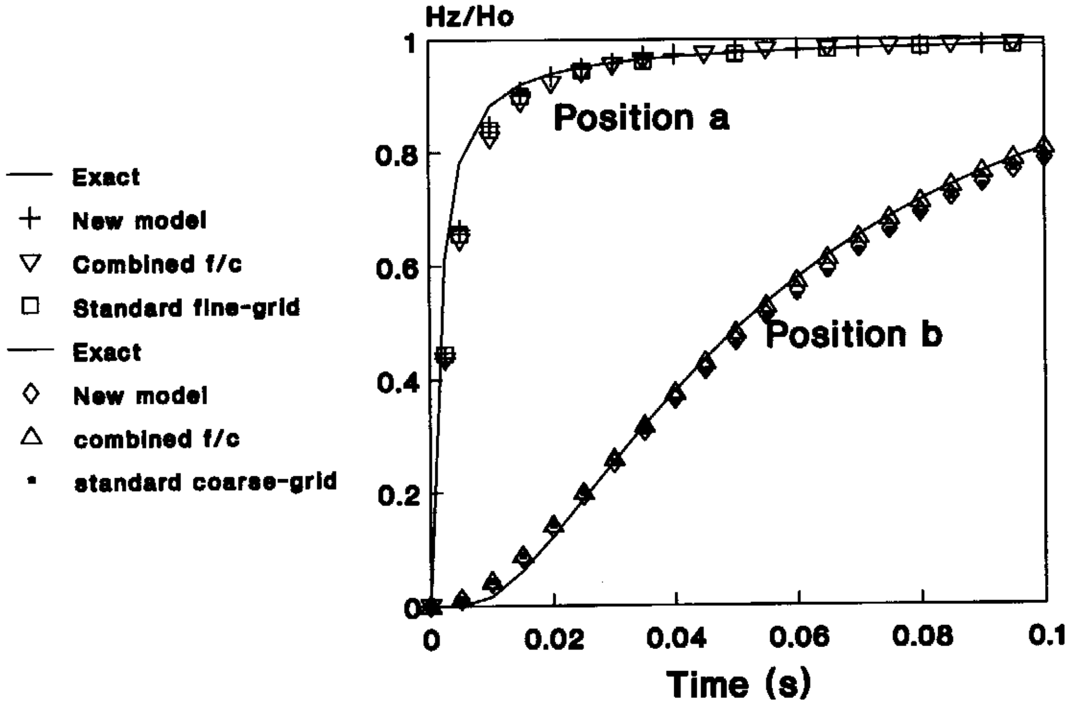

Figure 7 Flux penetration into a long square bar under an impact excitation (position "b" = "b_1").

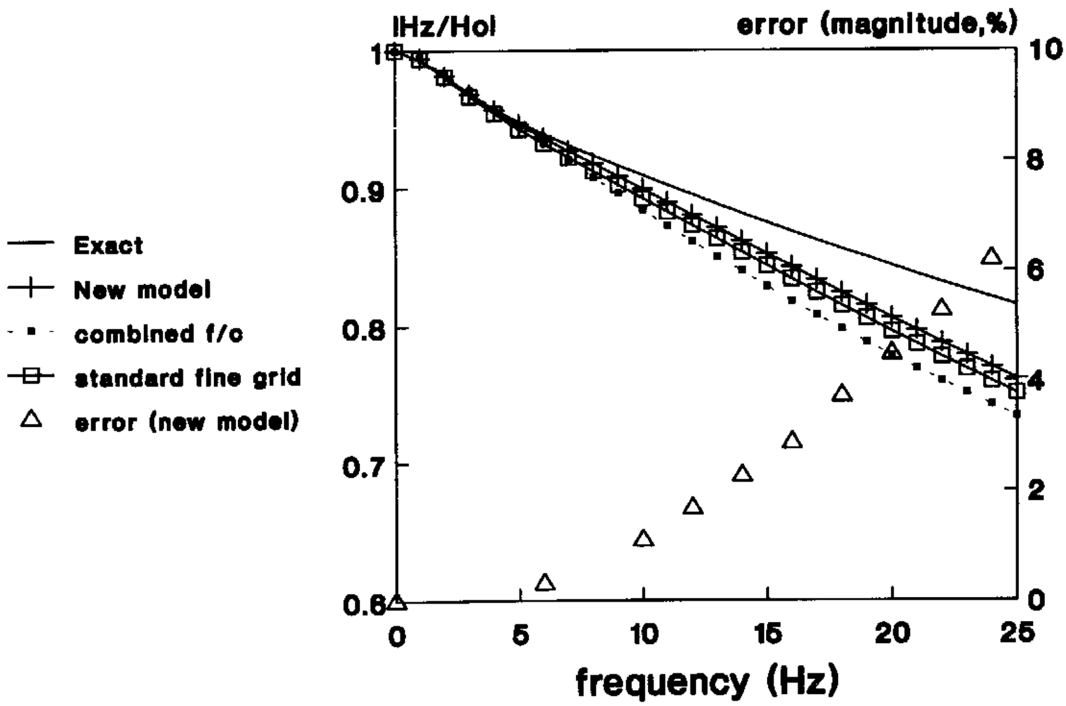

(a) Position "a" (h = W/8 and W = 1).

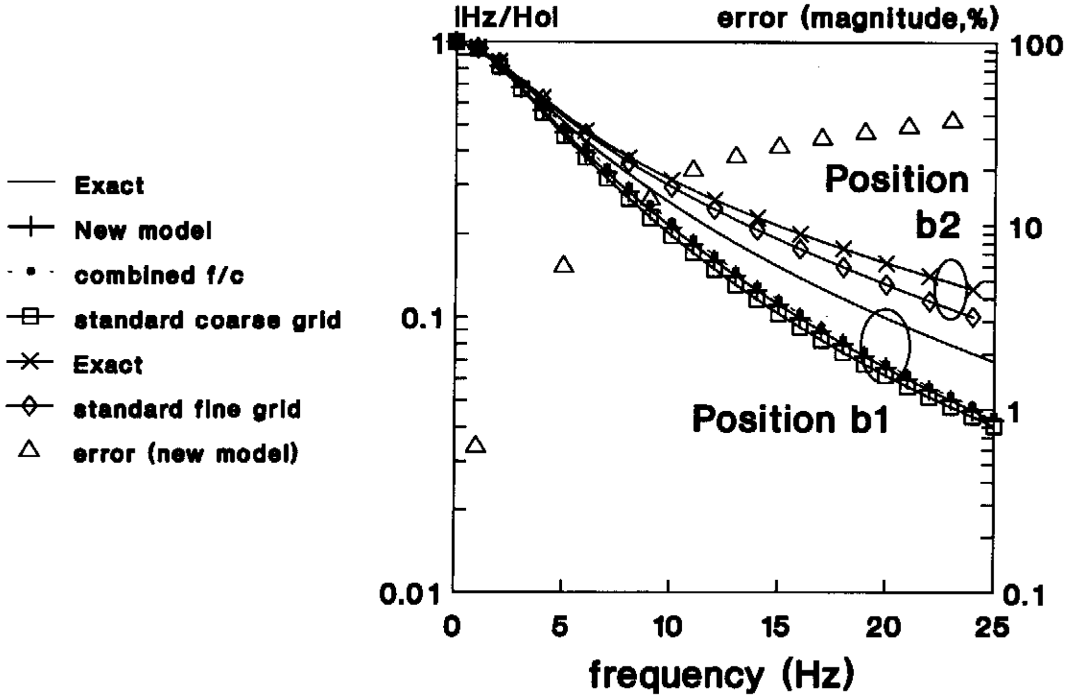

(b) Position "b_1" (h = W/4 and W = 1) and position "b_2" (h = W/8).

Figure 8 Frequency responses for the different network models at two representative positions. The horizontal axis can be converted to the dimensionless parameter $(h/\delta)^2$ by multiplying the factor πh^2, where δ is the skin depth.

	rms error,	(Position a)	
Freq. range (h/δ)	new model	combined fine-coarse	standard, with fine mesh
1 Hz to 20 Hz (0.222-0.992)	1.88%	3.96%	2.30%
1 Hz to 10 Hz (0.222-0.702)	0.29%	1.13%	0.84%

	rms error,	(Position b_1)	
Freq. range (h/δ)	new model	combined fine-coarse	standard, with coarse mesh
1 Hz to 20 Hz (0.443-1.984)	19.47%	17.78%	24.44%
1 Hz to 10 Hz (0.443-1.403)	9.12%	6.45%	12.88%

Table 1 Accuracy of various network models

3.2 Eddy current loss in a long square bar subjected to a transverse field

The third problem determines the eddy current loss in a long square bar excited by a transverse magnetic field. In this case, the electric field has one component (E_z) whereas the magnetic field has two (H_x and H_y). Maxwell's equations are:

$$-\frac{\partial Hx}{\partial y}+\frac{\partial Hy}{\partial x}=\varepsilon\frac{\partial Ez}{\partial t}+\sigma Ez$$
$$\frac{\partial Ez}{\partial y}=-\frac{\partial B}{\partial H}\frac{\partial Hx}{\partial t} \tag{7}$$
$$\frac{\partial Ez}{\partial x}=\frac{\partial B}{\partial H}\frac{\partial Hy}{\partial t}$$

The equivalence between network and field quantities is:

$$vz = Ez \;;\; ix = -Hy \;;\; iy = Hx \;;$$
$$l=\frac{\partial B}{\partial H} \;;\; c=\varepsilon \;\; and \;\; g=\sigma \tag{8}$$

The field in the vicinity of the bar is unknown and consequently the air region has to be solved. It is assumed that the field is unaffected by the presence of the bar in regions 2W from it. Other parameters used are:

$$\frac{\partial B}{\partial H}=\mu 0 \;;\; \varepsilon = \varepsilon 0 \;;\; W = 1\,cm$$
$$and \;\; \sigma = 10^7\; S/m\,(in\ conductor)$$
$$= 0\,(in\ free\ space) \tag{9}$$

For the frequency range used, the reactance of the shunt capacitor (C = εh) is at least 10 orders of magnitude larger than 1/(gh) or the reactance of *l*h. Therefore, the capacitors are assumed to be open-circuited. Due to symmetry, only one-quarter of the region is solved. In this case, the bar is covered with fine cells with h = 1/6 cm and the outer part of free space is covered with coarse cells. The power losses in per unit volume are determined in terms of P_o (power loss when δ = W/2 = 0.5 cm). The results are plotted in Figure 9. This problem involves two domains and is relatively large when compared with the previous two. The memory requirement recorded was approximately 130 k and the computing time was about 7.3 seconds on a standard 486 machine for 8 frequencies. As a comparison, results using a larger air region (4Wx4W) and results from reference 13 are included in Figure 9. SPICE3 running on a SUN workstation has been used for the former case. The interfacing busbar of the original combined fine-coarse mesh topology will force local potentials (= E_z) to be identical. In regions close to the boundary, where H_y is assumed constant, this assumption ($\partial E_z/\partial x$ = 0), along the x-direction, is unacceptable (see eq. (7)) and may produce erroneous results.

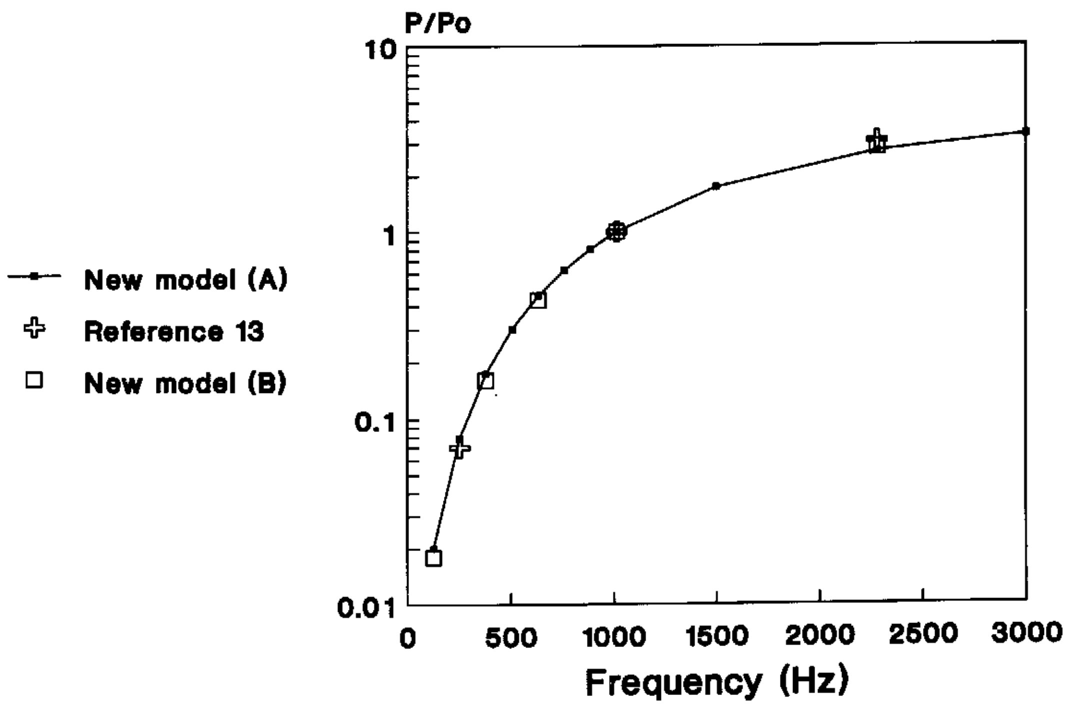

Fig. 9 Eddy current loss in a square bar due to a transverse magnetic field.
(A) - air region = 2Wx2W; (B) - air region = 4Wx4W.

The validity of this approach may be assessed by comparing adjacent node potentials around the interface between the fine- and coarse-cell. Consequently, the use of the original model must be exercised with care. On the other hand, the new model does not have this limitation.

4. CONCLUSIONS

This paper describes two network models for Maxwell's equations in two dimensions. The first model, which is based on the original combined fine-coarse mesh technique, is very straightforward to implement. However, it uses "busbars" at the fine- and coarse-cell interface and the resulting error may be unacceptable in some cases. In the new model the "busbars" are replaced by controlled sources and this problem is eliminated. Both models allow a reduction in the total number of cells within a field region to be modelled without compromising accuracy (this may be problem dependent for the original combined fine-coarse mesh technique) and can be easily solved by PSPICE, SPICE or other circuit simulators. Based on the new network analogues, field modellers can solve most two-dimensional field problems without the prior knowledge of numerical methods or the need of a dedicated software package.

5. REFERENCES

1. G. Kron, "Equivalent circuit of the field equations of Maxwell-I", *Proc. Inst. Radio Engr.*, **32**, 289-299 (1944).

2. J. Roberts, "Analogue treatment of eddy-current problems involving two-dimensional fields", *Proc. IEEE*, **107C**, 11-18 (1960).

3. P. Silvester, "Network Analog solution of skin and proximity effect problems", *IEEE Trans. Power Appar. Syst.*, **PAS-86**, 241-247 (1977).

4. J. Vine, "Impedance network", in *Field Analysis*, Vitkovitch (Ed.), Van Nostrand, London, 1966.

5. R. J. Lari and R. Turner, "Survey of eddy current programs", *IEEE Trans. Magnet.*, **MAG-19**, 2474-2477 (1983).

6. P. B. Johns, "A simple explicit and unconditionally stable numerical routine for the solution of the diffusion equation", *Int. j. numer. methods eng.*, **11**, 1307-1328 (1977).

7. S. Pulko, A. Mallik and P. B. Johns, "Application of transmission-line modelling (TLM) to the thermal diffusion in bodies of complex geometry", *Int. j. numer. methods eng.*, **23**, 2303-2312 (1986).

8. K. J. Binns and P. J. Lawrenson, *Analysis and computation of electric and magnetic field problems*, Part IV, Pergamon Press, Oxford, 1973.

9. W. Hackbusch and U. Trottenbery (Eds.), *Lecture Notes in Mathematics: Multigrid Methods II*, Springer-Verlag, New York, 1986.

10. R. E. Phillips and F. W. Schmidt, "Multigrid techniques for the numerical solution of the diffusion equation", *Num. Heat Transfer*, **7**, 251-268 (1984).

11. C. C. Wong, "Multigrid TLM for diffusion problems", *Int. j. numer. modelling*, **2**, 103-111 (1989).

12. R. Ait-Sadi, A. J. Lowery and B. Tuck, "Combined fine-coarse mesh transmission-line modelling method for diffusion problems", *Int. j. numer. modelling*, **3**, 111-126 (1990).

13. R. L. Stoll, *The analysis of eddy currents*, chapter 8, Clarendon Press, London, 1974.